"Physics of Auroral Phenomena", Proc. XLII Annual Seminar, Apatity, pp. 61-64, 2019

Polar
Geophysical
Institute

DOI: 10.25702/KSC.2588-0039.2019.42.61-64

ION KAPPA DISTRIBUTION PARAMETERS IN THE EQUATORIAL PLANE AT GEOCENTRIC DISTANCES SMALLER THAN 20 R_E AND AURORAL OVAL MAPPING TO THE EQUATORIAL PLANE

I.P. Kirpichev[1], E.E. Antonova[2,1], V.G. Vorobjev[3], O.I. Yagodkina[3], M.V. Stepanova[4], I.L. Ovchinnikov[2], M.S. Pulinets[2], S.S. Znatkova[2], N.V. Sotnikov[5], S.K. Mit'[2], P.S. Kazarian[5]

[1]*Space Research Institute (IKI) Russian Academy of Science, Moscow, Russia; e-mail: ikir@iki.rssi.ru*
[2]*Skobeltsyn Institute of Nuclear Physics, Moscow State University, Moscow, 119991, Russia;*
e-mail: elizaveta.antonova@gmail.com
[3]*Polar Geophysical Institute, Apatity, Russia*
[4]*University of Santiago de Chile, Chile*
[5]*Moscow State University, physical faculty*

Abstract. The improvement of the accuracy of the auroral oval boundaries mapping to the equatorial plane using the method of morphological mapping requires the determination of the ion pressure distributions at low latitudes and at the equatorial plane. To obtain exact values of pressure it is necessary to take into account the contribution of particles with energies much larger than energies of thermal particles. Particle distribution functions in the collisionless magnetospheric plasma are well approximated by kappa distributions. Kappa distributions have a Maxwellian core and power tails, and are characterized by three parameters: density, core energy/temperature and value k, which describes the spectral slope at energies much larger than thermal ones. Analyses of ion fluxes measured by the THEMIS mission allows us to obtain averaged distribution of kappa parameters of ions at the equatorial plane at geocentric distances from 7 to 20 R_E. We obtain the radial and MLT dependences of kappa parameters. The use of the obtained results for the specification of auroral oval mapping to the equatorial plane is discussed.

1. Introduction

The topology of the magnetospheric domains continues to be one of unsolved problems in magnetospheric physics. There are multiple works suggesting that the auroral oval is mapped to the plasma sheet, even though these suggestions are uncertain (see, *Kornilov et al.* [2008], *Antonova et al.* [2011]). Such mapping is based on magnetospheric magnetic field models with predefined current systems, and did not include all main current systems (see, *Antonova et al.* [2018a] and references therein). So, such models cannot produce the adequate auroral oval mapping. Analysis of the trapping boundary position relative to the auroral oval [*Riazantseva et al.*, 2018] shows that the trapping boundary of energetic electrons is localized inside the auroral oval. During a magnetic storm, trapping boundary can even coincide with polar boundary of the auroral oval [*Sotnikov et al.,* 2019]. Such findings show the inconsistency of the suggested auroral oval mapping to the plasma sheet with the results of experimental observations.

It was shown, that using the morphological method of auroral oval mapping [*Antonova et al.*, 2014, 2015, *Kirpichev et al.*, 2016] the main part of the quiet auroral oval is mapped to the outer part of the ring current (CRC in accordance with [*Antonova and Ganushkiva*, 1997, *Ganushkina et al.*, 2015, 2018]). The used method was based on the comparison of plasma pressure measurements at low altitudes and at the equatorial plane. The morphological method of auroral oval mapping requires the determination of plasma pressure distribution along the trajectory of auroral satellites. However, databases of many auroral missions contain results of particle measurements in limited energy ranges. For example, DMSP databases allows the obtaining ion spectra up to 30 keV and it is necessary to consider the high energy continuation of ion spectra for a correct obtaining of plasma pressure value. Such spectra at high latitude magnetosphere can be approximated by the kappa distribution function (see [*Livadiotis*, 2017] and references therein). Such approximations were used in many papers including the analysis of simultaneous THEMIS mission observations [*Stepanova and Antonova*, 2015] and statistical analysis of kappa distribution parameters during magnetospheric substorms [*Espinoza et al.*, 2018] in the limited sector near midnight $X_{GSM}<0$, $|Y_{GSM}| < |X_{GSM}|$, $|Z_{GSM}| < 8R_E$ from 7 up to 30 R_E,. Therefore, the results of *Espinoza et al.* [2018] can be used only for analysis of near midnight observations. For the analysis of the role of high-energy part of ion spectra in the calculation of plasma pressure at all MLT it is possible to use averaged kappa approximation of ion spectra at the equatorial plane obtained at all MLT.

Antonova et al. [2018b] describe the main features of kappa approximation analysis and present the results of such analysis in the daytime magnetospheric region. In this paper, we obtain the statistical results of such approximations at all MLT.

2. Instrumentation and data analysis

We used data of five satellite of the THEMIS mission available online (*http://themis.ssl.berkeley.edu/, http://cdaweb.gsfc.nasa.gov/*) [*Angelopoulos*, 2008; *Sibeck and Angelopoulos*, 2008]. Ion spectra were obtained by the electrostatic analyzer (ESA) [*McFadden et al*., 2008] and the solid state telescope (SST) [*Angelopoulos*, 2008]. We suggest that protons make the main contribution to the ion flux as ESA and SST instruments do not allow the determination of the ion composition, as it was shown that H^+ ions are the dominant ions during quite time intervals [*Daglis et al*., 1999]. The magnetic field measurements were done using the fluxgate magnetometer (FGM) [*Auster et al*., 2008] with a time resolution of 3 s. Full spectra were obtained using time and energy interpolation programs developed by the THEMIS team. We selected time intervals when ESA and SST devices worked with maximal energy and angle resolution (full regime). Due to low ion fluxes at high energies different times of spectra accumulation were used till ~10 min. Parameters of the solar wind were obtained using the Wind satellite data (*http://cdaweb.gsfc.nasa.gov/*), and the corresponding time shift due to propagation of the solar wind from the satellite location to the magnetopause was obtained using solar wind velocity data. We selected for the analysis very quiet periods when |Dst|<20 nT and |AL|<300 nT. Contamination from the spacecraft potential and photoelectrons at low energies set up the low energy limit of ion kappa approximation while energetic electrons and solar cosmic rays determine the high energy limit. Low statistics at high energies frequently prevent the use of high-energy channels. As a result, we included in the statistical analysis only robust averaged spectra. We determine three parameters of kappa approximation (see, *Antonova et al.* [2018b] for details): ion density n_0, k parameter determining high energy slope of ion spectra and core energy e_0, connected with thermal energy E_t by the relation $E_t=1.5e_0k(k-3/2)$.

3. Ion kappa distribution parameters at the equatorial plane in the GSM coordinate system

Fitting of ion spectra by a single kappa distribution function is made in a limited energy range. Fig. 1 shows examples of kappa approximations of measured spectra at geocentric distances L~9, L~6 and L~4. As it can be seen, the obtained fits differ significantly. The energetic inner ring current ions (L~ 4 R_E) have energetic rigid high energy spectrum, which corresponds to low values of kappa, and high values of core energy. At greater distances, the spectra are softer and closer to Maxwellian ones. At the latitudes of equatorial boundary of auroral oval during quiet time periods at L~6-7 the shape of the distribution function is far from Maxwellian distribution, which is necessary to take into account calculating the plasma pressure values.

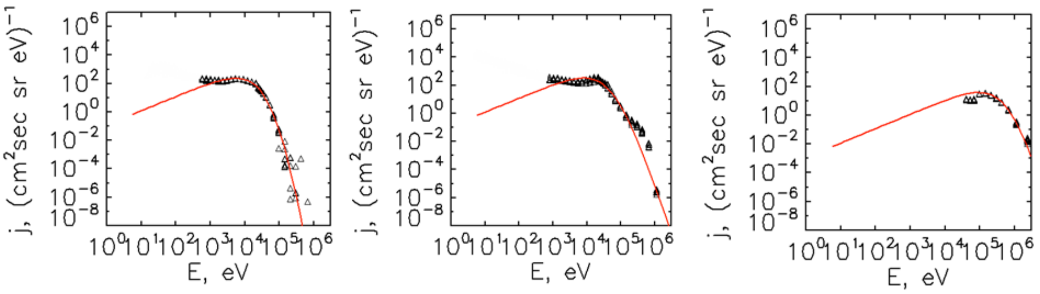

L ~ 9 L ~ 6 L ~ 4

Figure 1. Examples of kappa approximations of the measured spectra.

Fig. 2 shows the global distribution of the n_0 parameter of kappa approximation (ion density) at the equatorial plane (Fig. 2a) and the averaged dependence of n_0 value on the radial distance for night, morning, evening and day sectors of the magnetosphere (Fig. 2b). It is possible to see that the MLT dependence of kappa parameter n_0 is comparatively weak during quiet geomagnetic conditions. However, it is possible to clearly identify a surrounding the Earth plasma ring at all MLT with ion density close to ion density in the plasma sheet.

Fig. 3 shows the global distribution of thermal energy E_t (Fig. 3a) and averaged dependence of the e_0 value on radial distance at four selected MLT sectors (the same as in Fig. 2). Figure three shows the clear transition from the plasma domain, corresponding to traditional ring current at geocentric distances <5 R_E with averaged energy ~50-100 keV, to the outer part of the ring current with averaged energy ~10 keV.

Fig. 4 shows the global distribution of the k parameter (Fig. 4a) and averaged dependence of the k value on radial distance at four selected MLT sectors (the same as in Fig. 2). It is possible to see the increase of this parameter with the increase of geocentric distance with the formation of plateau (practical absence of dependence) at a geocentric distance larger than 10 R_E.

Region from 5 to 7 R_E are shown on Figs. 2-4a and is absent in Figs. 2-4b. Such feature is explained by the averaging of the global distribution of kappa parameters, which produce picture smearing. Indeed, the statistics of ion spectra approximated by single kappa function in the 5-7 region is much smaller than the number of single kappa approximations at larger and smaller distances. Most spectra in this transitional region can be approximated by bikappa distributions. We consider such feature as the possible result of the equatorial part of auroral oval mapping to the equatorial plane where the ionosphere is a power source of upward accelerated ionospheric ions, which add the ion populations with different characteristics.

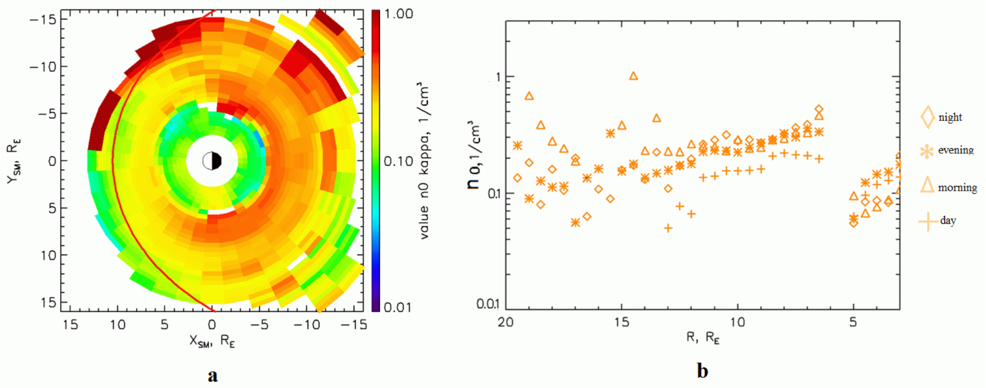

a b

Figure 2. Distribution of the n_0 parameter at the equatorial plane (***a***) and dependence of n_0 on radius for different sectors (***b***).

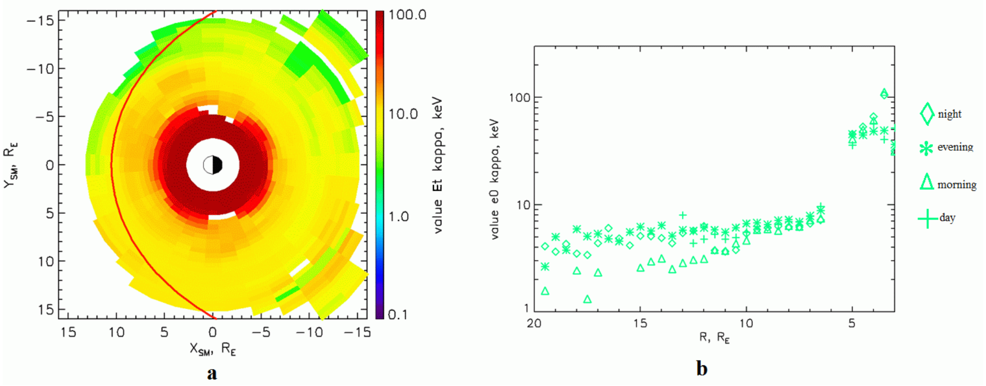

a b

Figure 3. Distribution of E_t at the equatorial plane (***a***) and dependence of e_0 on radius for different sectors (***b***).

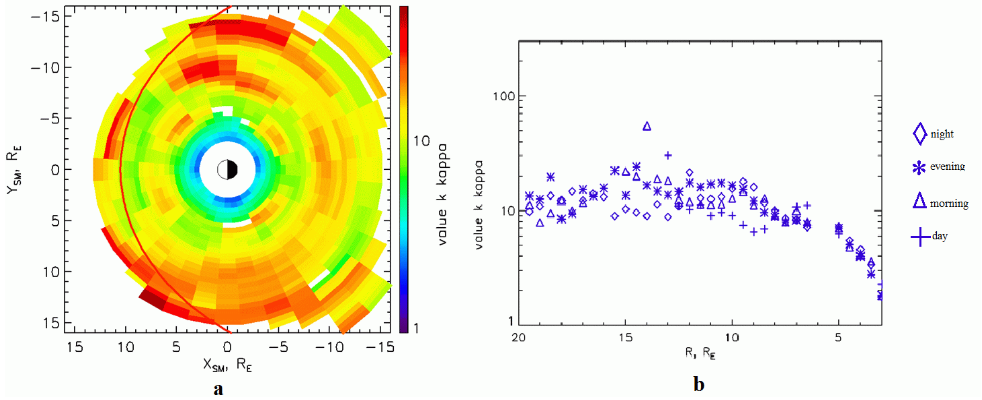

a b

Figure 4. Distribution of the k parameter at the equatorial plane (***a***) and dependence of k on radius for different sectors (***b***).

4. Conclusions and discussion

We analyzed the distribution of parameters of ion spectra approximation at the equatorial plane by single kappa function using data of the THEMIS mission. Obtained pictures are in agreement with previously obtained results of using kappa approximations for the analysis of magnetospheric processes. Obtained pictures at all MLT sectors support the concept of auroral oval mapping to the surrounding the Earth plasma ring and show a number of new features, which require more careful analysis. Our results show that it is necessary to take into account kappa approximation for calculation of plasma pressure in the equatorial part of auroral oval, where the auroral oval is overlapped with traditional ring current and the k parameter is comparatively small (hard ion spectra).

Acknowledgements. We acknowledge the members of THEMIS teams for the use of data. The work is supported by the grant of the Russian Foundation for Basic Research No 18-05-00362.

References

Angelopoulos, V. (2008), The THEMIS mission, *Space Sci. Rev.*, *141*, 5–34, doi:10.1007/s11214-008-9336-1.

Antonova, E.E., and N.Yu. Ganushkina (1997), Azimuthal hot plasma pressure gradients and dawn-dusk electric field formation, *Journal of Atmospheric and Terrestrial Physics*, *59*, 1343–1354, doi:10.1016/S1364-6826(96)00169-1

Antonova, E.E., I.P. Kirpichev, I.L. Ovchinnikov, et al. (2011), *IAGA Special Sopron Book Series. Vol. 3. The Dynamic Magnetosphere*, Ed. by W. Liu and M. Fujimoto, 201-210, doi:10.1007/978-94-007-0501-2.

Antonova, E.E., V.G. Vorobjev, I.P. Kirpichev, and O.I. Yagodkina (2014), Comparison of the plasma pressure distributions over the equatorial plane and at low altitudes under magnetically quiet conditions, *Geomag. Aeron. 54*(3), 278-281, doi:10.1134/S0016793214030025.

Antonova, E.E., V.G. Vorobjev, I.P. Kirpichev, O.I. Yagodkina, and M.V. Stepanova (2015), Problems with mapping the auroral oval and magnetospheric substorms, *Earth, Planets, and Space 67*, 166, doi:10.1186/s40623-015-0336-6.

Antonova, E.E., M.V. Stepanova, I.P. Kirpichev, I.L. Ovchinnikov, V.G. Vorobjev, O.I. Yagodkina, M.O. Riazanseva, V.V. Vovchenko, M.S. Pulinets, S.S. Znatkova, and N.V. Sotnikov (2018a), Structure of magnetospheric current systems and mapping of high latitude magnetospheric regions to the ionosphere, *Journal of Atmospheric and Solar-Terrestrial Physics*, *177,* 103-114, doi: 10.1016/j.jastp.2017.10.013.

Antonova, E.E., M.V. Stepanova, I.P. Kirpichev et al. (2018b), Kappa distributions and feature of magnetospheric dynamics, *"Physics of Auroral Phenomena", Proc. XLI Annual Seminar, Apatity,* 42-45, doi:10.25702/KSC.2588-0039.2018.41.42-45.

Auster, H.U., et al. (2008), The THEMIS fluxgate magnetometer, *Space Sci. Rev.*, *141*, 235–264, doi:10.1007/s11214-008-9365-9.

Daglis, I.A., R.M. Thorne, W. Baumjohann, and S. Orsini (1999), The terrestrial ring current: origin, formation, and decay, *Rev. Geophys. 37*, 407–438, doi:10.1029/1999RG900009.

Espinoza, C.M., M.V. Stepanova, P.S. Moya, E.E. Antonova, and J.A. Valdivia (2018), Ion and electron k -distribution functions along the plasma sheet. *Geophys. Res. Lett., 45*(13), 6362-6370, doi:10.1029/2018GL078631.

Ganushkina, N.Y., M.W. Liemohn, S. Dubyagin, I.A. Daglis, I. Dandouras, D.L. De Zeeuw, et al. (2015), Defining and resolving current systems in geospace, *Ann. Geophys.*, *33*, 1369–1402, doi:10.5194/angeo-33-1369-2015.

Ganushkina, N.Y., M.W. Liemohn, and S. Dubyagin (2018), Current systems in the Earth's magnetosphere. *Reviews of Geophysics*, *56*(2), 309-332, doi:10.1002/2017RG000590.

Kirpichev, I.P., O.I. Yagodkina, V.G., Vorobjev, E.E. Antonova (2016), Position of projections of the night side auroral oval equatorward and poleward edges in the magnetosphere equatorial plane*, Geomagn. Aeron.* 56, 407–414, doi:10.1134/S001679321604006X.

Kornilov, I.A., E.E. Antonova, T.A. Kornilova, and O.I. Kornilov (2008), Fine structure of auroras during auroral breakup according to the ground-based and satellite observations, *Geomag. Aeron.,* 48(1)*,* 7–19, doi:10.1134/S00167932080100.

Livadiotis, G. (2017), Kappa distributions: theory and applications in plasmas. Elsevier. Amsterdam, Oxford, Cambridge. MA. oCLC: 990766561.

McFadden, J.P., C.W. Carlson, D. Larson, J. Bonnell, et al. (2008), THEMIS ESA first science results and performance issues, *Space Sci. Rev.*, *141*, 477–508, doi:10.1007/s11214-008-9433-1.

Sibeck, D.G., and V. Angelopoulos (2008), THEMIS science objectives and mission phases, *Space Sci. Rev.*, *141*, 35–59, doi:10.1007/s11214-008-9393-5.

Riazanteseva, M.O., E.E. Antonova, M.V. Stepanova, B.V. Marjin, I.A. Rubinshtein, V.O. Barinova, N.V. Sotnikov (2018), A relation between the locations of the polar boundary of outer electron radiation belt and the equatorial boundary of the auroral oval, *Ann. Geophys., 36*, 1131–1140, doi 10.5194/angeo-36-1131-2018.

Sotnikov, N.V., E.E. Antonova, M.O. Ryazantseva, V.O. Barinova, I.A. Rubinshtein*a*, and S.K. Mit' (2019), Position of the energetic electron trapping boundary relative to auroral oval boundaries during the magnetic storm on December 19–22, 2015, based on data from the Meteor-M2 Satellite, *Geomag. Aeron.,* 59(2)*,*136-146, doi:10.1134/S0016793219020142.

Stepanova, M., and E.E. Antonova (2015), Role of turbulent transport in the evolution of the κ distribution functions in the plasma sheet, *J. Geophys. Res. Space Physics*, *120*, 3702–3714, doi:10.1002/2014JA020684.

Wing, S., and P.T. Newell (1998), Central plasma sheet ion properties as inferred from ionospheric observations, *J. Geophys. Res., 103*(A4), 6785-6800, doi:10.1029/97JA02994.